Eksakta : Berkala Ilmiah Bidang MIPA
VOLUME 26 NO 01 2025, pp 50-61
ISSN : Print 1411-3724 — Online 2549-7464
DOI : https://doi.org/10.24036/eksakta/vol26-iss01/530

Eksakta
Berkala Ilmiah Bidang MIPA
http://www.eksakta.ppj.unp.ac.id/index.php/eksakta

Article

Preparation and Analysis of Dual-Property Coated Metal Foams for Potential Wick Structures in Heat Pipe Applications

Doli Bonardo [1*], Hollanda Arief Kusuma[1], Muhammad Tanveer[2], Budi Dharma[3], Fauzan Amri[4]

[1]Department of Electrical Engineering, Faculty of Maritime Engineering and Technology, Universitas Maritim Raja Ali Haji, Tanjungpinang, Indonesia
[2]Department of Physics, Faculty of Science, University of Gujrat, Gujrat, Pakistan
[3]Refrigeration and Air Conditioning Engineering, Politeknik Tanjungbalai, Tanjungbalai, Indonesia
[4]Instrumentation and Control Engineering Technology, Politeknik Negeri Indramayu, Lohbener, Indonesia

Article Info

Article history :

Received July 11, 2024
Revised December 20, 2024
Accepted January 06, 2025
Published Maret 30, 2025

Keywords :
Metal foam, hydrophilic coating, hydrophobic coating, heat pipe, wick structure

Abstract. Hydrophilic and hydrophobic coated metal foams have been successfully prepared via a cleaning procedure and a simple spraying technique to be used as a wick structure in a heat pipe. The main object of this work is to explore the effect of hydrophilic and hydrophobic layers on the metal foam and to study the properties of the metal foams. To achieve this goal, 3D-OM analyses were performed to identify the pore size of the metal foam. To observe the surface morphology and porosity of the metal foam, SEM analysis was carried out and succeeded in observing the changes in the surface roughness of the hydrophilic and hydrophobic coated metal foams. The pore diameter, porosity and density of metal foam were 633.38 µm, 48.46% and 4.62 g/cm3, respectively. FT-IR analysis was also performed with the results showing that the hydrophobic coating did not affect the overall molecular group composition. Contact angle analysis shown that the values were 74° and 112° (first day) on the hydrophilic and hydrophobic coated samples.

Corresponding Author :
Doli Bonardo
Department of Electrical Engineering, Faculty of Maritime Engineering and Technology, Universitas Maritim Raja Ali Haji, Tanjung Pinang, Indonesia
Email: dolibonardo@umrah.ac.id

1. Introduction

Electronic components and devices now stand at the heart of technological innovation, driving progress in both overt and subtle ways. Every type of electronic and mechanical operation produces energy utilized by humans in daily activities. According to the conservation of energy principle, all energy forms that have been converted result in other energy forms, maintaining the total amount of energy even though it is not completely transformed into the desired form. One common by-product of these energy conversions is heat energy, which is widely distributed in nature. Although usually an unwanted by-product, heat energy has significant potential for conversion into more useful forms. However, if not properly managed, excess heat energy can disrupt system performance and potentially lead to complete system failure [1-2].

The discovery of the heat pipe has been a major breakthrough in managing thermal issues. These small devices, known for their high heat transfer efficiency and conductivity, utilize rapid phase changes from liquid to vapor and back to liquid within the evaporator and condenser, respectively [3]. Heat pipes have been integrated into various technological applications, including electronic device cooling, heat pumps, CPU cooling systems, solar heaters, LEDs, and two-phase thermal control systems. Additionally, different types of heat pipes, such as straight heat pipes, loop heat pipes (LHPs), and ultra-thin heat pipes, have been developed to meet specific needs [4].

A critical component in heat pipes is the wick structure, which facilitates the flow of the working fluid, enabling efficient heat transfer [5]. An ideal wick structure should exhibit superior material and physical properties, such as a small contact angle with water to maximize capillary action, low thermal resistance, and high thermal conductivity. These properties are essential for optimizing heat pipe performance, ensuring efficient heat transfer, and maintaining temperature stability at hot spots [6]. In addition, this structure must also have low thermal resistance and high thermal conductivity. Materials that have the above advantages are needed to be applied as a wick structure on heat pipes to maximize their performance in delivering and absorbing heat while also maintaining temperature stability at hot spots [7].

Metal foam has emerged as a promising material for wick structures due to its high porosity, which supports rapid and optimal fluid and heat distribution. Commercially available metal foam is used in various applications, from soundproofing in households to orthopedic, automotive, and energy-absorbing components in the manufacturing industry [8]. Its excellent thermal energy absorption properties make it a strong candidate for heat pipe wick structures.

Various studies on the use of metal foam as a wick structure in heat pipes have been carried out to analyze its performance before and after modification treatments such as the difference in heat flux applied [4], the difference in pores per inch (PPI) and coating with super hydrophobic materials [5]. In addition, Shi and colleagues in 2020 have also carried out scientific evidence regarding different methods and chemical modifications can produce variations in the adhesion properties of metal foams so that they offer different heat pipe performance. Metal foam with 30 PPI has been analyzed for its ability by modifying the surface layer using a hydrophobic layer [9], and the specification of 15 PPI is currently still not studied regarding its material characteristics and physical properties. The gap in current research lies in the limited understanding of the material characteristics and physical properties of 15 PPI metal foam, particularly after surface modification treatments. Addressing this gap is urgent to enhance the performance of heat pipes, especially for applications requiring precise thermal management.

In this research, the metal foam sample will be prepared and coated with 3-layer super hydrophobic liquid to analyze its effect on the physical properties and characteristics of the material. Physical testing and material characterization of metal foam is expected to provide basic scientific insight as a reference for application as a wick structure material in heat pipes.

This research aims to prepare and coat 15 PPI metal foam with a three-layer superhydrophobic liquid to analyze its effect on the material's physical properties and characteristics. Through physical testing and material characterization, this study seeks to provide fundamental scientific insights that could serve as a reference for applying 15 PPI metal foam as a wick structure in heat pipes, thereby advancing the field of thermal management technology. By exploring the uncharted territory of 15 PPI metal foam's potential in heat pipe applications, this research endeavors to contribute to more efficient and effective thermal management solutions, reinforcing the crucial role of innovative materials in technological progress.

2. Experimental Section

The metal foam (15 PPI) used in this investigation was a commercial type produced by Recemat BV, Netherlands. Supernano hydrophobic liquid repellent brand No Wet and acetone from Sigma-Aldrich were utilized. For sample preparation, the metal foam samples were cut to dimensions of 32.7 mm in length, 8.2 mm in width, and 7.3 mm in height. To prepare the surface for both hydrophilic and hydrophobic layers, the metal foam was smoothed using sandpaper, then immersed in acetone for 20 minutes to clean and remove any dirt. Following the acetone bath, the samples were dried in an oven at 110 °C for 15 minutes and allowed to cool to room temperature inside the oven. For the hydrophobic coating application, the cleaned and dried metal foam samples were sprayed with Supernano hydrophobic liquid repellent in three repetitions, with a 20-minute interval between each spray to ensure a uniform coating.

Subsequent characterization of the samples involved both physical testing and material analysis. Physical testing included measuring porosity, pore size distribution, and overall surface morphology. Several characterizations were analyzed in this investigation, including a 3D Optical Microscope INSIZE 5301-D400 for detailed surface inspection, SEM-EDX with a JEOL type JSM – 6390A for surface morphology and elemental analysis, and Fourier-transform infrared spectroscopy (FTIR) using a Perkin Elmer Spectrum Two for identifying functional groups. Additionally, contact angle and capillary analysis were performed to assess the hydrophobicity and fluid transport properties of the coated metal foam surfaces.

3. Results and Discussion

3.1. 3D-Optical Microscope

Figures 1a and 1b show a three-dimensional morphological image of the metal foam and its pore size distribution. Based on the analysis using the ImageJ application, the average pore diameter is 633.38 μm, with a total of 15 pores per inch (PPI). These measurements align with previous research [9] indicating that an increase in the number of pores in a metal foam of the same size results in a smaller average pore size. However, the pore size distribution reveals a variety of size variations. Using a Gaussian method approach, the distribution of pore sizes in the metal foam samples exhibits a normal distribution pattern. This implies that half of the total pore sizes are smaller than the average pore size, while the other half are larger. Larger pore sizes can decrease liquid capillary pressure, which may reduce the thermal performance of the heat pipe when metal foam (15 PPI) is used as a wick structure.

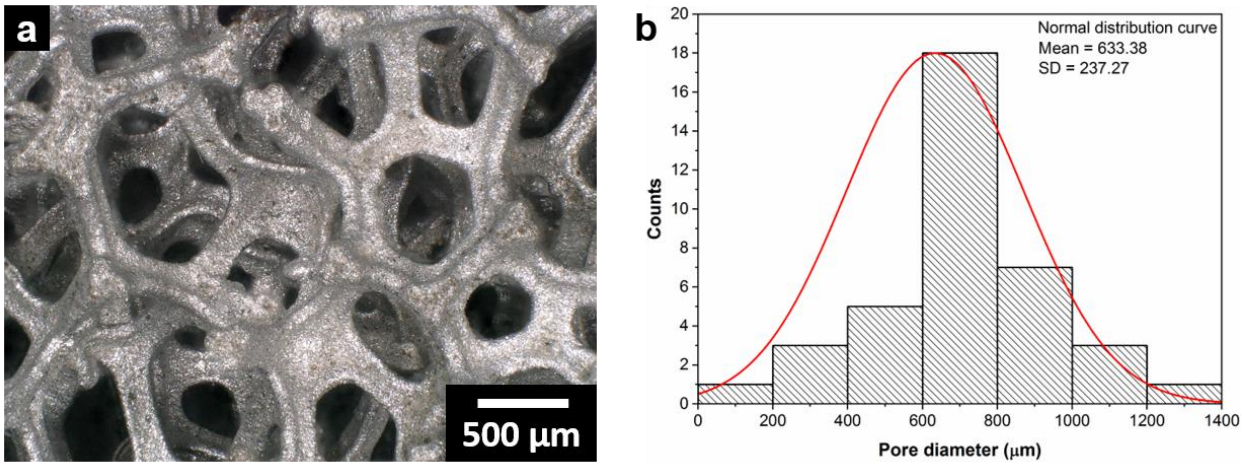

Figure 1. 3D OM image of metal foam (a) and pore diameter distribution (b)

3.2. Pore Characteristic

Table 1 presents the porosity values and the number of pores per inch (PPI) in this study compared with those from a previous study. The average density of the metal foam is 4.62 g/cm³. The hydrophobic coating does not significantly affect this density value due to the inherent characteristics of the metal foam. The coating maintains the basic composition of the material, as it does not involve significant chemical reactions. Consequently, the pore texture of the metal foam remains unchanged by the hydrophobic layer [10]. However, if the hydrophobic layer applied to the metal foam surface were thick enough to fill the cavities, it could potentially alter the foam's density. Despite this, the porosity values remain relatively consistent, indicating that the pore structure of the metal foam does not undergo significant shrinkage or expansion.

Table 1. Porosity and number of pores per inch metal foam

No.	Sample	Pore per inch (PPI)	Porosity (%)	Ref.
1	Stainless steel foam	15	48.46	This work
2	Stainless steel foam	30	92	[11]
3	Aluminum foam	10	88	[12]
4	Copper foam	15	95	[13]
5	Copper foam	35	97	

3.3. Surface Morphology

Figure 2 shows the SEM image of the sample with a hydrophilic layer and with a hydrophobic layer. As it can be seen that through 500 times magnification, the sample of hydrophilic layer has a fairly even distribution of grain pores. In addition, through the 2000x magnification, it is seen that the solid surface is smoother and cleaner. This situation is somewhat different from the hydrophobic layer with the same magnification, because the surface of the grains is seen to be covered with other grains adhering to the surface.

The hydrophobic layer on the metal foam surface increases the roughness level so that its morphology looks rough compared to hydrophilic metal foam [14]. The surface roughness factor is a function of physical dimensions that can increase the surface area so that there is a gradual change in the surface chemistry of metal foam, so the wettability level is reduced. High porosity in metal foam samples is a characteristic that is not shared by other types of materials [15]. The high porosity supports the provision of an optimal active surface [16-17]. This porosity plays a very important role in

supporting the fluid distribution, so that the capillarity that occurs in the pore crevices increases. The results of research conducted by Shin and colleagues in 2018, which states that metal foam has a large air volume compared to other materials so that the base metal content is only present in the pore nodes [18].

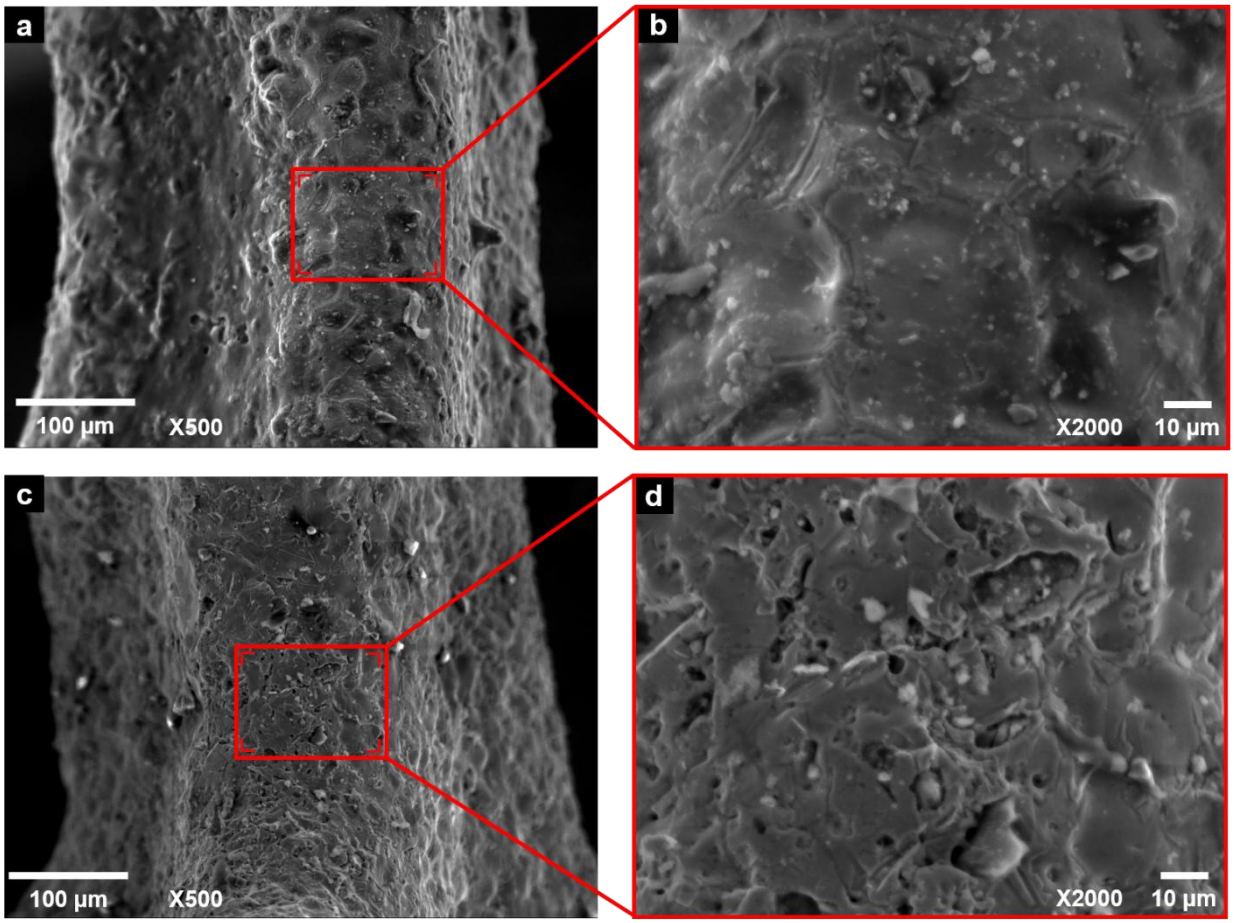

Figure 2. SEM morphology: (a) metal foam with hydrophilic layer (X500), (b) metal foam with hydrophilic layer (X2000), (c) metal foam with hydrophilic layer (X500), and (d) metal foam with hydrophobic layer (X2000)

Figures 3 and 4 show EDX spectra which provide an overview of the elements that make up metal foams of hydrophilic and hydrophobic layers, respectively. The hydrophilic metal foam sample was dominated by chromium (Cr), iron (Fe) and nickel (Ni) elements. However, the element chromium still ranks highest in terms of the dominant content of the entire spectral point. The hydrophobic layer produces silicon (Si) elements in the metal foam. Hydrophobic layers are made of special polymers that may contain oxygen atoms so that they are trapped with the main atoms of the constituent elements of the metal foam [19].

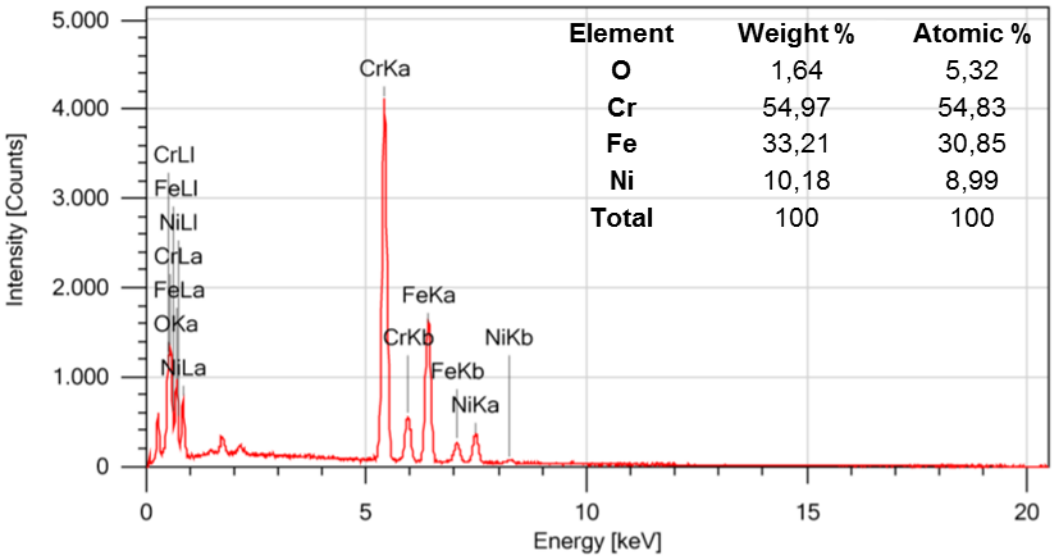

Figure 3. EDX spectra of metal foam with hydrophilic layer

Research by Brennan and coworkers stated that the additive layer on the metal foam surface traps the oxygen molecules entering the interior of the surface because it undergoes a catalysis process when reacting with the catalyst additive layer [20]. However, this result still needs to be investigated further considering that the hydrophobic layer has non-volatile properties so that the content of some chemical atoms will depend on time. This is because the longer the metal foam with a hydrophobic layer is left on its surface, the more likely it will experience other chemical reactions on its surface.

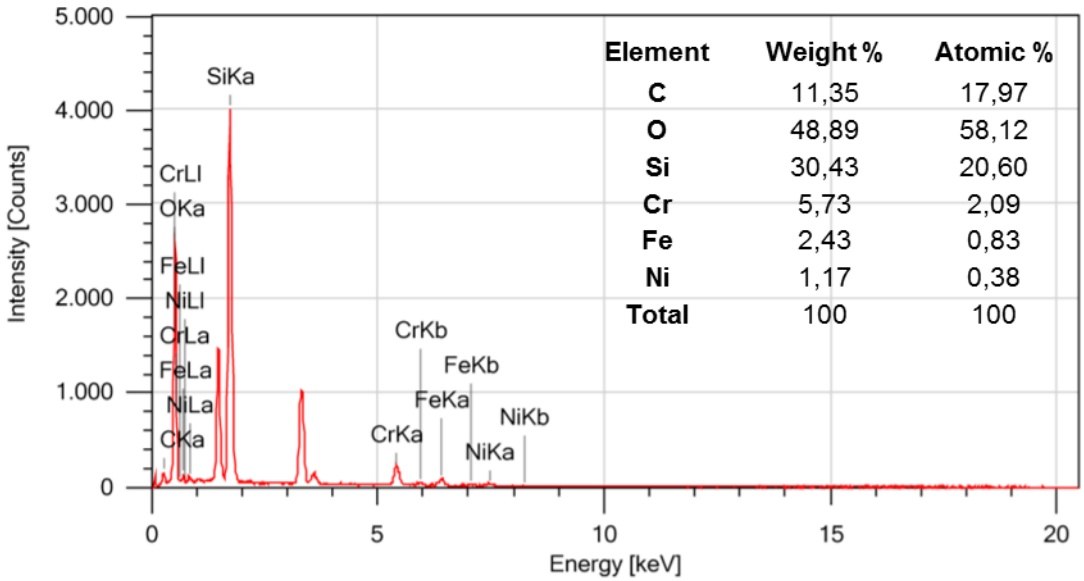

Figure 4. EDX spectra of metal foam with hydrophobic layer

3.4. FT-IR Analysis

Fourier-transform infrared spectroscopy (FTIR) spectrum was observed to investigate the chemical composition and for the study of different functional groups present in the hydrophobic as surface layer [21]. Figure 5 shows the FTIR pattern formed on the hydrophilic metal foam and the hydrophobic metal foam. Samples with the hydrophobic layers had an identical FTIR wave patterns to the hydrophilic layers. This is because the reaction between the metal foam and the hydrophobic layer does not take place molecularly [22]. However, there is a new peak that was previously not indicated as a peak with a wave number of 1004.68 which indicates a low-intensity Si-O-Si group. The content of SiO_2 was detected in the surface layer of metal foam on samples with the hydrophobic layers. When viewed from the analysis of the elements contained in the metal foam, the pores of the granules were identified as containing the element oxygen (O) while the metal foam granules contained the element chromium (Cr), however this was not the result of a chemical reaction between the hydrophobic and metal foam particles because there is no heat energy to support chemical reactions. This shows that the hydrophobic coating does not affect the overall molecular group composition.

Figure 7 illustrates the curve depicting the relationship between electrical conductivity values and frequency function for all samples. It can be observed that the electrical conductivity values of the CGG sample range from 10^{-7} to $3.75x10^{-7}$ S.cm^{-1} and increase to the range of $6x10^{-4}$ to $1.4x10^{-3}$ S.cm^{-1} for the CGG-C sample. This indicates that the addition of 6% CNT by the total mass of the CGG polymer composite supports the development of its electrical conductivity properties inside composite polymer structure [23-24].

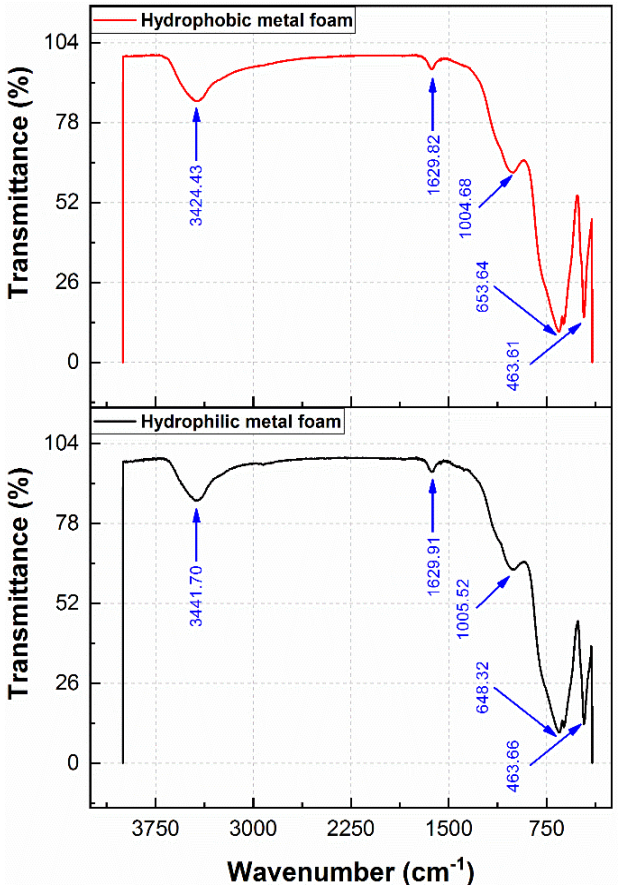

Figure 5. Fourier transform infrared spectroscopy (FTIR) spectra of hydrophilic and hydrophobic coated metal foam.

3.5. Contact Angle Analysis

The contact angle test was carried out to determine the tendency of the metal foam sample when its surface is in direct contact with water so that identification of the adhesion properties of the metal foam can be achieved. The contact angle can also be used to check the surface quality of metal foam samples that have been coated with the coating material. There are four possibilities that will occur in these conditions, which will be hydrophobic, hydrophilic, super hydrophobic or super hydrophilic [25]. The behavior of water droplets on the metal foam surface is shown in Figure 6. Metal foam without a hydrophobic layer shows hydrophilic properties on the first day to day 5, while from day 10 to day 15 the metal foam surface is hydrophobic. Figure 8 shows the contact angle on the metal foam surface with a hydrophobic coating. From the first day to the 15th day, the surface of the metal foam is hydrophobic, even on the 15th day it can be categorized as super hydrophobic.

The wettability of the hydrophilic metal foam was more stable when compared to samples with a hydrophobic layer. This indicates that the amount by which a liquid, in this case water molecules, can spread over the sample surface is determined by the intermolecular forces between the surface and the liquid. Based on the analysis of the physical properties of the two samples, it can be confirmed that the sample of the hydrophilic metal foam has the most optimum level of capillarity and is supported by its hydrophilic characteristics with a contact angle on the first day of 74° making it possible to use it as a wick structure in heat pipes [26-27].

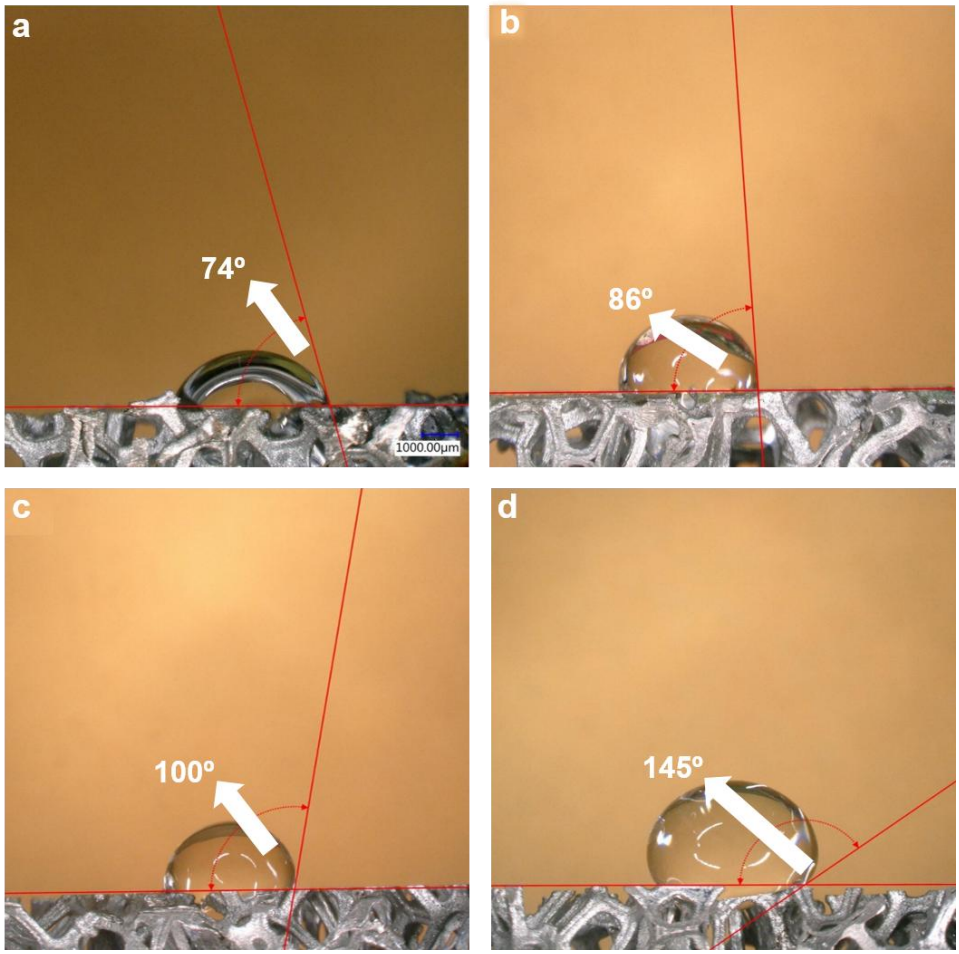

Figure 6. Contact angle of hydrophilic metal foam surface on day 1 (a), day 5 (b), day 10 (c) and day 15 (d).

Figure 6 shows the contact angle between water and the hydrophilic metal foam surface during the time range from the first day to the 15th day. On the first day to the fifth day, the hydrophilic metal foam had a contact angle of less than 90°, on the 10th to 15th day the adhesion level decreased, this was indicated by the measured contact angle exceeding 90°. The presence of the acetone liquid helps to support the attractive bonds between the metal foam particles and water [28], but over time, the acetone liquid evaporates and disappears so that the attractive force between the metal foam particles and water decreases. This condition is certainly not expected for the material that is applied as a wick structure on the heat pipe which must have good adhesion to the working fluid in order to enhance its performance [29-30].

The contact angle between water and the metal foam surface with hydrophobic layers during the time range from the first day to the 15th day is shown in Figure 7. Metal foam with hydrophobic layers showed hydrophobic properties since the first day of contact angle measurement, and increased contact angle on the next day until the 15th day. The hydrophobic layer causes the surface roughness of the metal foam to increase, thus affecting its adhesion properties. In the wick structure heat pipe application, metal foam with a low contact angle will support a good heat transfer process because of its adhesion, so that the attraction between the fluid and the metal foam is higher than that of the fluid particles [6].

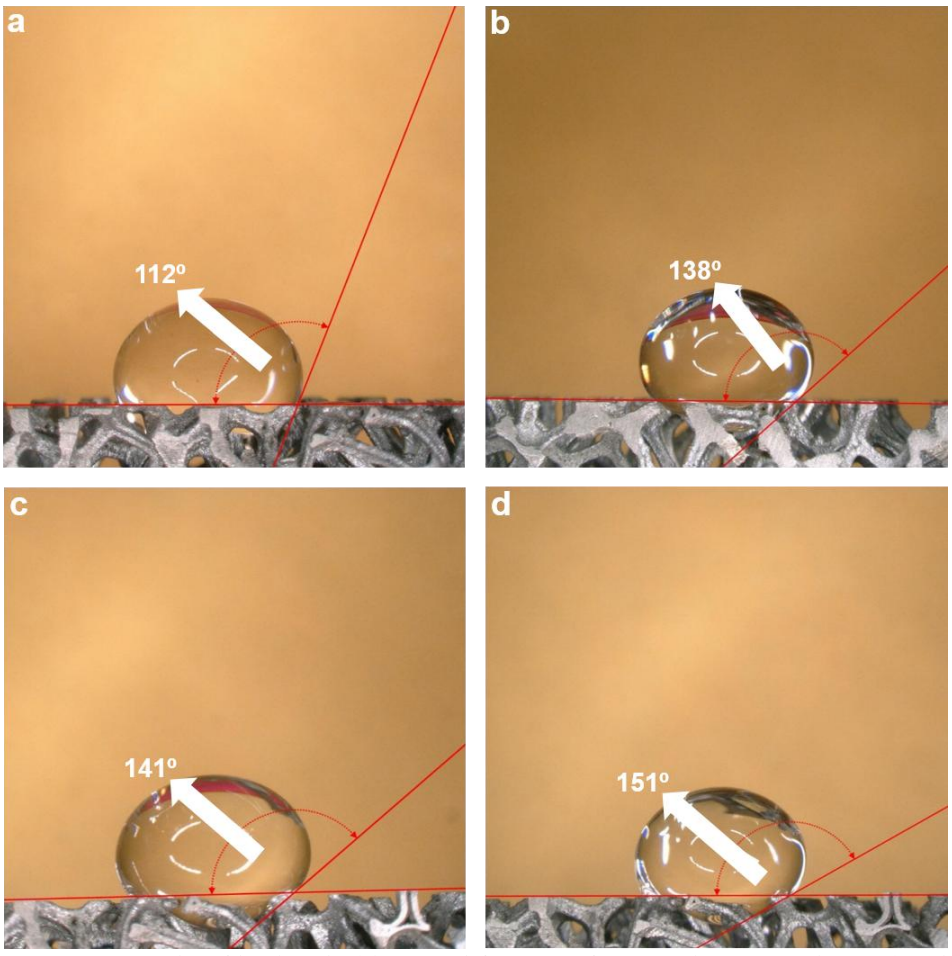

Figure 7. Contact angle of hydrophobic metal foam surface on day 1 (a), day 5 (b), day 10 (c) and day 15 (d).

3.6. Capillarity

Figure 8 illustrates the relationship between the mass of distilled water absorbed by the metal foam capillary structure and the time elapsed. Capillary pumping measurements commence as soon as the bottom of the sample contacts the surface of the distilled water. Initially, the rate of capillary pumping increases rapidly within the first few seconds. Metal foam without hydrophobic coatings absorbs 0.012 grams of water in the initial 10 seconds, maintaining stability for the subsequent 35 seconds. After 90 seconds, the capillary saturation is achieved, indicated by maximum water absorption. In contrast, the hydrophobic-coated metal foam absorbs 0.03 grams of distilled water within the first 10 seconds and continues at this rate for the next 50 seconds. After 90 seconds, the capillary pumping also reaches saturation, with no additional movement of water as it fills the capillary spaces to their maximum capacity. The hydrophobic coating on the metal foam impairs its capillary action by decreasing the material's affinity for water [31-32].

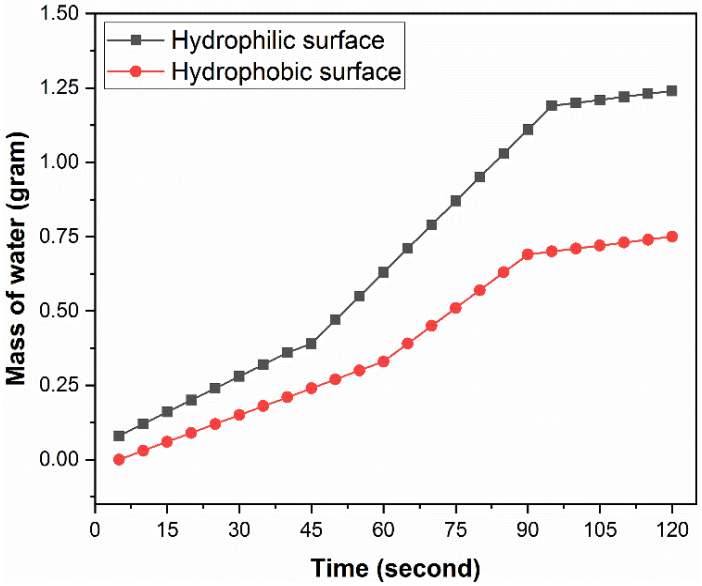

Figure 8. Time vs mass curve of water on the capillary properties of hydrophilic and hydrophobic metal foam

4. Conclusion

Metal foam with and with hydrophobic and hydrophilic layers were prepared by spraying technique and acetone treatment. The variety of pore sizes shows a variation in diameter with a normal distribution. Metal foam 15 PPI has a porosity of 48.46 % and a density of 4.62 g/cm^3. The surface roughness of hydrophobic metal foam is the reason that causes a decrease in wettability or weakening of the interfacial bond between water and solid metal foam, because roughness is a physical dimension factor that increases the contact surface area so that it easily traps air which can increase contact heterogeneity that occurs on the metal foam surface. The additive layer on the metal foam surface traps the oxygen molecules entering the interior of the surface because it undergoes a catalysis process when it reacts with the catalyst additive layer. In addition, the hydrophobic coating did not affect the overall molecular group composition. The wettability of hydrophilic metal foam layer was more stable when compared to samples with hydrophobic layers. Hydrophobic coated metal foam inhibits its capillary ability because it reduces the level of adhesion of metal foam to water.

References

[1] He, Z., Yan, Y., & Zhang, Z. (2021). Thermal management and temperature uniformity enhancement of electronic devices by micro heat sinks: A review. *Energy*, *216*, 119223.

[2] Rostamian, F., Etesami, N., & Haghgoo, M. (2021). Management of electronic board temperature using heat sink containing pure and microencapsulated phase change materials. *International Communications in Heat and Mass Transfer*, *126*, 105407.

[3] Yan, B. H., Wang, C., & Li, L. G. (2020). The technology of micro heat pipe cooled reactor: A review. *Annals of Nuclear Energy*, *135*, 106948.

[4] Luo, J. L., Mo, D. C., Wang, Y. Q., & Lyu, S. S. (2021). Biomimetic copper forest wick enables high thermal conductivity ultrathin heat pipe. *ACS nano*, *15*(4), 6614-6621.

[5] Nugraha, P. F., & Putra, N. (2019). The fabrication and testing development of heat pipe wicks: A review. In *2019 IEEE 2nd International Conference on Power and Energy Applications (ICPEA)* (pp. 264-271). IEEE.

[6] Tetuko, A. P., Nurdiyansah, L. F., Addin, M., Setiadi, E. A., Ginting, M., & Sebayang, P. (2020). Magnetic nanofluids as heat transfer media in heat pipes. *Advances in Natural Sciences: Nanoscience and Nanotechnology*, *11*(2), 025002.

[7] Cui, Z., Jia, L., Wang, Z., Dang, C., & Yin, L. (2022). Thermal performance of an ultra-thin flat heat pipe with striped super-hydrophilic wick structure. *Applied Thermal Engineering*, *208*, 118249.

[8] Cui, W., Li, X., Li, X., Lu, L., Ma, T., & Wang, Q. (2022). Combined effects of nanoparticles and ultrasonic field on thermal energy storage performance of phase change materials with metal foam. *Applied energy*, *309*, 118465.

[9] Ginting, F. H., Humaidi, S., & Tetuko, A. P. (2022). Stainless steel foam as wick material in heat pipe for electronics cooling application. In *Journal of Physics: Conference Series* (Vol. 2193, No. 1, p. 012025). IOP Publishing.

[10] Lee, S., Tam, J., Li, W., Yu, B., Cho, H. J., Samei, J., ... & Erb, U. (2019). Multi-scale morphological characterization of Ni foams with directional pores. *Materials Characterization*, *158*, 109939.

[11] Kaya, A. C., Zaslansky, P., Ipekoglu, M., & Fleck, C. (2018). Strain hardening reduces energy absorption efficiency of austenitic stainless steel foams while porosity does not. *Materials & Design*, *143*, 297-308.

[12] Bağcı, Ö., Arbak, A., De Paepe, M., & Dukhan, N. (2018). Investigation of low-frequency-oscillating water flow in metal foam with 10 pores per inch. *Heat and Mass Transfer*, *54*, 2343-2349.

[13] Ali, H. M. (2018). Experimental investigation on paraffin wax integrated with copper foam based heat sinks for electronic components thermal cooling. *International Communications in Heat and Mass Transfer*, *98*, 155-162.

[14] Croll, S. G. (2020). Surface roughness profile and its effect on coating adhesion and corrosion protection: A review. *Progress in organic Coatings*, *148*, 105847.

[15] Sembiring E, Bonardo D, Sembiring K and Sitorus Z. (2021). Analyze The Strength of Ceramics Made from Clay, Sinabung Volcanic Ash and Sea Water in The Term of The Structure. *Journal of Physics: Conference Series*, *2019* 012066.

[16] Bonardo D, Septiani N L W, Amri F, Estananto, Humaidi S, Suyatman and Yuliarto B. (2021). Review—Recent Development of WO 3 for Toxic Gas Sensors Applications. *Journal of The Electrochemical Society*, *168* 107502.

[17] Manetti, L. L., Ribatski, G., de Souza, R. R., & Cardoso, E. M. (2020). Pool boiling heat transfer of HFE-7100 on metal foams. *Experimental Thermal and Fluid Science*, *113*, 110025.

[18] Alvandifar, N., Saffar-Avval, M., & Amani, E. (2018). Partially metal foam wrapped tube bundle as a novel generation of air cooled heat exchangers. *International Journal of Heat and Mass Transfer*, *118*, 171-181.
[19] Kim, K., Lichtenhan, J. D., & Otaigbe, J. U. (2019). Facile route to nature inspired hydrophobic surface modification of phosphate glass using polyhedral oligomeric silsesquioxane with improved properties. *Applied Surface Science*, *470*, 733-743.
[20] Brennan M C, Keist J S and Palmer T A. (2021). Defects in Metal Additive Manufacturing Processes. *Journal of Materials Engineering and Performance*, *30* 4808–18.
[21] Sajjad M, Ullah I, Khan M I, Khan J, Khan M Y and Qureshi M T. (2018). Structural and optical properties of pure and copper doped zinc oxide nanoparticles. *Results in Physics*, *9* 1301–9.
[22] Cheng J, Li Y, Zhong J, Lu Z, Wang G, Sun M, Jiang Y, Zou P, Wang X, Zhao Q, Wang Y and Rao H. (2020). Molecularly imprinted electrochemical sensor based on biomass carbon decorated with MOF-derived Cr2O3 and silver nanoparticles for selective and sensitive detection of nitrofurazone. *Chemical Engineering Journal*, *398* 125664.
[23] Vandghanooni S and Eskandani M. (2019). Electrically conductive biomaterials based on natural polysaccharides: Challenges and applications in tissue engineering. *International Journal of Biological Macromolecules*, *141* 636–62.
[24] Wang Y and Weng G J. (2018). Electrical Conductivity of Carbon Nanotube- and Graphene-Based Nanocomposites. *Micromechanics and Nanomechanics of Composite Solids* (Cham: Springer International Publishing) pp 123–56
[25] Ahmad D, van den Boogaert I, Miller J, Presswell R and Jouhara H. (2018). Hydrophilic and hydrophobic materials and their applications. *Energy Sources, Part A: Recovery, Utilization, and Environmental Effects*, *40* 2686–725.
[26] Egbo M, Keese J and Hwang G. (2021). Enhanced wickability of bi-particle-size, sintered-particle wicks for high-heat flux two-phase cooling systems. *International Journal of Heat and Mass Transfer*, *179* 121714.
[27] Jafari D, Di Marco P, Filippeschi S and Franco A. (2017). An experimental investigation on the evaporation and condensation heat transfer of two-phase closed thermosyphons. *Experimental Thermal and Fluid Science*, *88* 111–23.
[28] Ningrum, R. A., Humaidi, S., Sihotang, S., & Bonardo, D. (2022). Synthesis and material characterization of calcium carbonate (CaCO3) from the waste of chicken eggshells. In *Journal of Physics: Conference Series* (Vol. 2193, No. 1, p. 012009). IOP Publishing.
[29] Xie D, Sun Y, Wang G, Chen S and Ding G. (2021). Significant factors affecting heat transfer performance of vapor chamber and strategies to promote it: A critical review. *International Journal of Heat and Mass Transfer*, *175* 121132.
[30] Dai Y, Zhang R, Qin Z, Liu K, Liu C and Zhao J. (2024). Research on the thermal performance and stability of three-dimensional array pulsating heat pipe for active/passive coupled thermal management application. *Applied Thermal Engineering*, *245* 122793.
[31] Li H, Fu S, Li G, Fu T, Zhou R, Tang Y, Tang B, Deng Y and Zhou G. (2018). Effect of fabrication parameters on capillary pumping performance of multi-scale composite porous wicks for loop heat pipe. *Applied Thermal Engineering*, *143* 621–9.
[32] Lu, N., Li, J., & Liu, F. (2022). Experimental study on gradient pore size capillary wicks. *Heat Transfer Research*, *53*(7).